ELSEVIER

Journal of Crystal Growth 213 (2000) 135–140

JOURNAL OF CRYSTAL GROWTH

www.elsevier.nl/locate/jcrysgro

Ice configuration near a growing ice lens in a freezing porous medium consisting of micro glass particles

Kunio Watanabe[a,*], Masaru Mizoguchi[b]

[a]*Nougyo-Doboku, Faculty of Bioresources, Mie University, 1515 Kamihama Chyo, Tsu 514-8507, Japan*
[b]*Department of Biological and Environmental Engineering, The University of Tokyo, Tokyo 113-8657, Japan*

Received 28 December 1999; accepted 17 February 2000
Communicated by T. Nishinaga

Abstract

To observe the formation of ice lenses, unidirectional freezing experiments were carried out using a water-saturated porous medium made from micro glass particles. Knowledge of the ice configuration in the vicinity of a growing ice lens is important for clarifying the mechanism of the formation of ice lenses. The ice configuration in the vicinity of the warmest ice lens in the freezing porous medium was investigated by combining Raman spectroscopy with the unidirectional freezing experiments. No ice was found in any pore, warmer than the ice lens and the ice lens grows without penetrating the warmer pores. © 2000 Elsevier Science B.V. All rights reserved.

PACS: 81.10.A; 68.35.R; 64.70.D; 47.55.M

Keywords: Ice lens; Raman spectroscopy; Unidirectional freezing; Porous medium; Glass particles

1. Introduction

When porous media consisting of water and fine particles, such as soil, are frozen unidirectionally, the water sometimes forms regions of ice that are almost devoid of particles [1,2]. These regions are called ice lenses, and repetition of the process results in the formation of intermittent layers of ice lenses. The formation of ice lenses is recognized as a necessary condition for frost heave.

To clarify the mechanism of the formation of ice lenses, it is important to observe the configuration of ice in freezing porous media. Kumai [3] observed the ice configuration in frozen clay by scanning electron microscopy. Colbeck [4] directly observed the freezing front in a water saturated, unconsolidated medium consisting of glass beads a few millimeters in diameter. These observations, however, dealt only with freezing porous media in which ice lenses did not form. Some models of the formation of ice lenses in freezing soil emphasize the importance of ice growing in the frozen fringe, which was assumed to consist of a network of pore ice extending from the base of the warmest ice lens to a position at or near the 0°C isotherm [5–7]. Direct observation of the ice configuration in the

* Corresponding author. Tel.: + 81-59-232-1211, ext. 2377; fax: + 81-59-231-9571.
E-mail address: kunio@dobokupc4.bio.mie-u.ac.jp (K. Watanabe).

PII: S0022-0248(00)00353-5

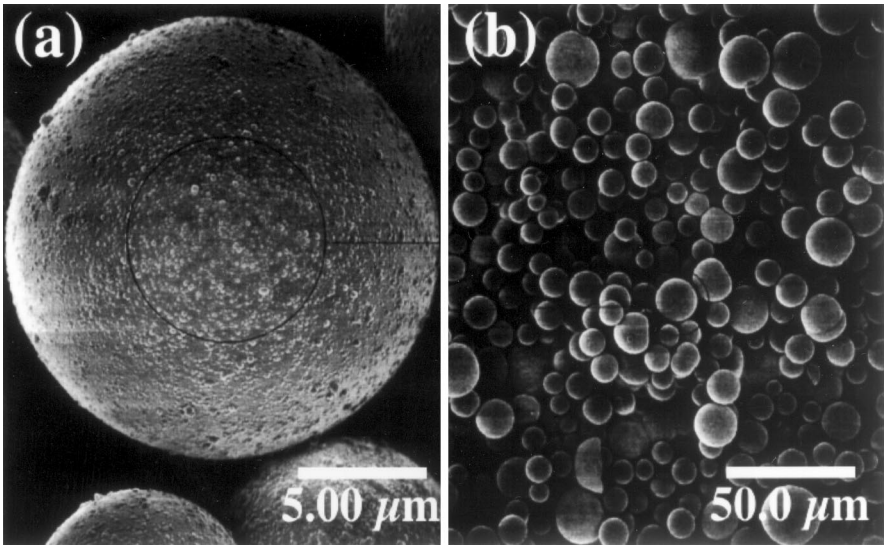

Fig. 1. Electron micrographs of glass particles. The micrograph (a) is 10 times the magnification of (b).

vicinity of a growing ice lens, however, has not yet been carried out.

In this study, we present the results of in situ observations of ice lenses in a unidirectionally freezing porous medium consisting of water and micro glass particles. The ice configuration in the vicinity of a growing ice lens is revealed from the Raman spectra of the water-saturated pores formed by glass particles near the ice lens.

Table 1
Characteristics of the glass particles prepared

Mean diameter of particle (μm)	9.7
Mean diameter of nanopore (nm)	3.3
Specific nanopore volume (cm^3/g)	0.30
Specific surface area (m^2/g)	150.5
Specific gravity of particle (g/cm^3)	2.12
Dry powder density (g/cm^3)	0.791
Water content (g H_2O/g SiO_2)	0.790

2. Experimental procedures

2.1. Sample

The porous medium that we used consisted of Vycor glass particles, which formed a fine powder. Fig. 1 shows electron micrographs of a sample. The particles were spherical with roughly the same diameters and their surface had nano-pores with a uniform diameter. Table 1 shows some characteristics of the sample. The mean diameter of the particles was estimated from the electron micrographs. The mean diameter of the nano-pores and the specific surface area were determined by nitrogen adsorption. Fig. 2 shows the liquid water fraction in the

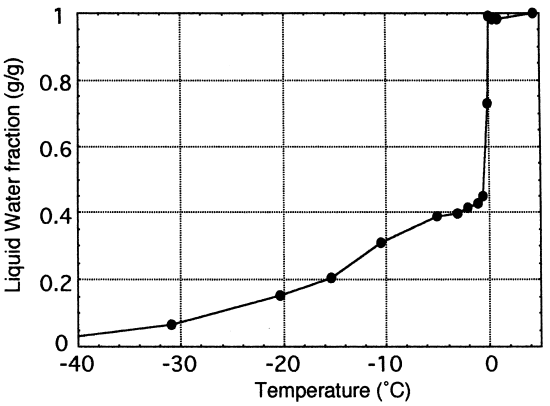

Fig. 2. Liquid-water fraction in the frozen porous medium measured by NMR technique.

frozen sample measured using an NMR technique, which accurately measures the liquid water fraction in porous media [8]. Since all the water melt, the liquid water fraction of unfrozen sample remains a constant value. More than 0.4 g/g of the water did not freeze at -1°C. This large amount of unfrozen water will come from its high specific surface area and presence of nanopores.

The water used was distilled, deionized and degassed. Water-saturated porous medium was prepared by placing the glass particles in a desiccator with water, evacuating the desiccator, allowing a few days for the solid–vapor equilibrium to be established, adding liquid water, and allowing the system to equilibrate for a day. The prepared sample was placed into a sample cell, which consisted of two $26 \times 76 \times 1\,mm^3$ glass slides and acrylic spacers, and sealed with silicone, except for a small hole on one side to relieve pressure. The inside volume of the sample cell was $20 \times 70 \times 3\,mm^3$. Two copper-constantan thermocouples with a diameter of 0.3 mm, calibrated with an accuracy of 0.03°C, were inserted into the sample cell to measure the temperature. Before the unidirectional freezing experiment, the cell was initially cooled to 2°C.

2.2. Unidirectional freezing

The sample was frozen using the unidirectional freezing apparatus shown in Fig. 3, which is basically the same as that designed by Nagashima and Furukawa [9]. The sample cell was placed in a Teflon cell holder. The opposite ends of the cell were held at different temperatures, T_H and T_L, by using two copper blocks kept at constant temperatures by Peltier thermoelements. This established a temperature gradient in the sample cell. A microscope equipped with a charge-coupled device camera and video tape recorder system was placed above the cell and used to observe a growing ice lens. Images of a growing ice lens were captured at 1 min intervals. A computer divided the images into a 20-μm grid and the growth rate of the ice lens was determined from the relative coordinates of the growth surface. The temperature profile was traced on the image using the locations and temperatures of the thermocouples, which were a few millimeters apart and sandwiched the growth surface. The temperature at the growth surface was estimated from the temperature profile.

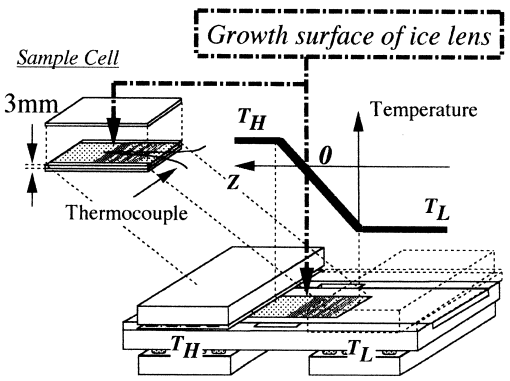

Fig. 3. Schematic illustration of the unidirectional freezing apparatus. A temperature gradient is established along the Z-axis.

2.3. Raman spectroscopy

The Raman spectrum arising from translational lattice vibrations in ice Ih shows a molecular-optic band peak at $225\,cm^{-1}$ [10,11]. If ice exists, this peak should be observed. While the warmest ice lens was growing, water in the vicinity of the growth surface was investigated using a Raman spectroscope (JOBIN YVON RAMANOR T64000), which was placed above the sample cell. The Raman spectroscope was calibrated to $0.1\,cm^{-1}$ by recording the standard emission lines of neon. This instrument was equipped with a charge coupled device detector that allows simultaneous recording of the frequency range between 50 and $400\,cm^{-1}$. The excitation energy for Raman emission was produced by an Argon ion laser using monochromatic radiation of 514.5 nm with an output of 150 mW. The spectral resolution was $0.45\,cm^{-1}$ for all spectra. The incident laser beam was focused on a spot of the freezing sample 1 μm in diameter, under a microscope. The time elapsed during each measurement was 30 s. Since the ice lenses we observed grew less than 0.5 μm during each measurement, we neglected the growth of the ice lens during the measurement period.

3. Results and discussion

3.1. Ice lenses in a porous medium consisting of glass particles

When different temperatures were applied to either end of the sample cell, ice lenses formed, as shown in Fig. 4. The black and white areas in Fig. 4 are ice lenses and glass particles, respectively. An ice lens initially appeared near the cold end of the sample cell and grew with time. Once the ice lens had grown a few 100 μm, it stopped growing and a new ice lens then appeared in a place warmer than where the previous ice lens was growing. Consequently, the ice lenses formed intermittent layers perpendicular to the direction of heat flow, which is from right to left in Fig. 4. The ice lenses that formed later were thicker. Fig. 5 shows the change in the thickness of the ice lens that formed at the warmest place in the sample. The elapsed time was counted from the beginning of formation of the warmest ice lens. Initially, the warmest ice lens grew rapidly, and then grew more slowly. After 300 min, the warmest ice lens was 1.2 mm thick. The temperature gradient near the warmest ice lens was $0.25^{\circ}C\,mm^{-1}$ and the temperature at the growth surface of the ice lens was estimated to be $-0.06^{\circ}C$.

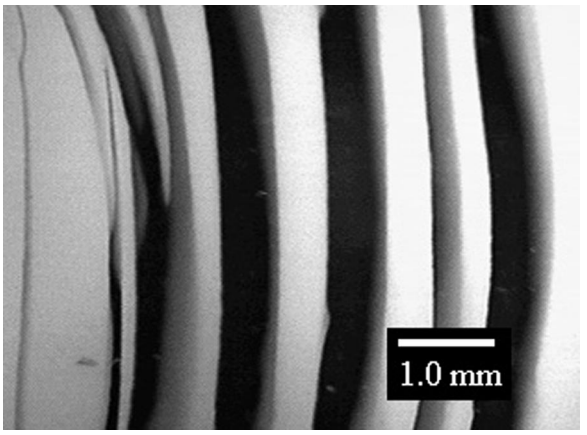

Fig. 4. Ice lenses in the porous medium consisting of glass particles. Right-hand side is colder and left-hand side is warmer. The ice lenses appears black since background can be seen through the ice lenses, and the porous medium appear white. The ice lenses grew from cold side and formed intermittent layers in the direction perpendicular to heat flow.

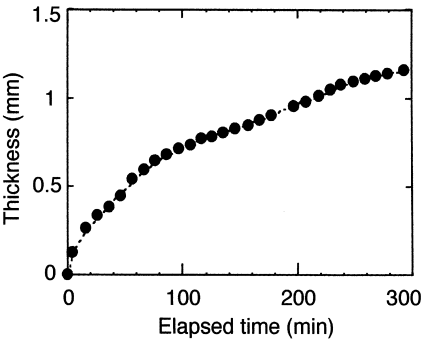

Fig. 5. Thickness of the warmest ice lens with time.

3.2. Raman spectra of water near the warmest ice lens

In order to evaluate the influence of the sample cell and glass particles on the Raman spectra, preliminary experiments were carried out using samples at room temperature and the temperature of liquid nitrogen. No remarkable peaks arising from the sample cell and the glass particles were observed in the frequency range between 50 and $400\,cm^{-1}$ from either sample (Fig. 7, R_{Room} and R_{LN}).

Then, we measured the Raman spectra to observe the peak at $225\,cm^{-1}$ in the vicinity of an ice lens that had grown for 300 min. Fig. 6(a) shows a computer-processed image of the vicinity of the growth surface of the ice lens monitored using the Raman system. The right side is colder and the left side is warmer. The warmest ice lens appears black, and the glass particles appear as white circles. To measure each pore, the diagnostic spot was moved in 0.4-μm steps, as shown in Fig. 6(b), where d is the distance from the growth surface of the warmest ice lens.

Fig. 7 shows a series of the Raman spectra obtained from pores at distance d. The spectrum in the ice lens ($d < 0$) had a strong peak at $225\,cm^{-1}$, which indicated the existence of ice Ih. The peak was also observed in the spectrum at the boundary between a glass particle and the ice lens ($d = 0$). On the other hand, the spectrum at a warmer pore more than 5 μm away from the ice lens ($d > 5$) had no remarkable peak at $225\,cm^{-1}$, and was very similar to that of the sample at room temperature (R_{Room}).

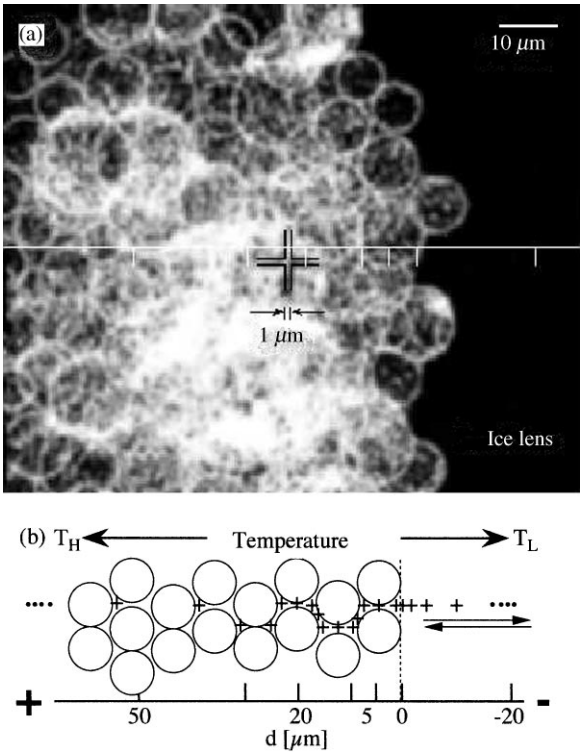

Fig. 6. (a) Computer-processed image and (b) schematic illustration of the vicinity of the growth surface of the warmest ice lens monitored using the Raman system. The diagnostic spot was moved in 0.4-μm steps for the measurement of each pore as shown in (b), where d is distance from the growth surface of the warmest ice lens.

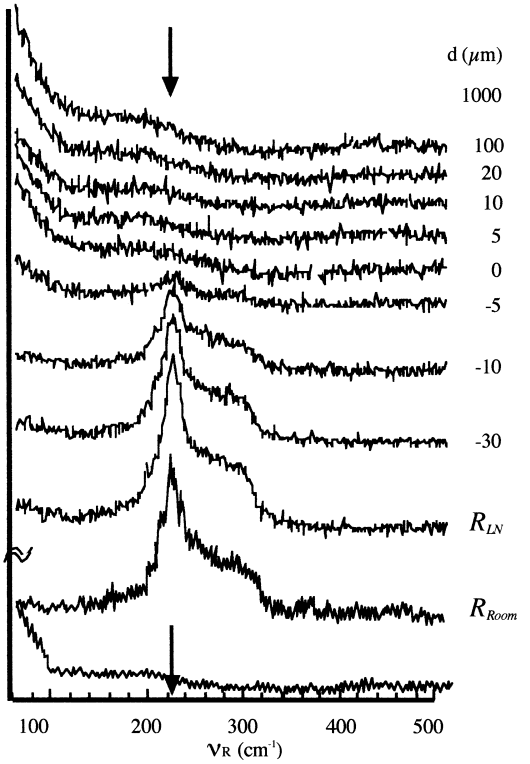

Fig. 7. Raman spectra of pore water in the vicinity of the warmest ice lens. d is distance from the growth surface of the warmest ice lens in Fig. 6(b). R_{Room} and R_{LN} are the Raman spectra of samples at room temperature and the temperature of liquid nitrogen, respectively.

3.3. Ice configuration and profile near the warmest ice lens

If enough water reaches the growth surface of an ice lens, the ice lens will keep growing. If there is not enough water, however, the ice lens will stop growing and another ice lens will start to form in a new location. Therefore, water near the growth surface is important for ice lens formation. In our experiment, no ice larger than 1 μm was observed in pores at locations warmer than the ice lens. In nucleation, only aggregates larger than a critical size are stable and grow to become the solid phase. The size of the aggregates depends on the temperature and decreases with the temperature. Assuming a cylindrical solid in liquid at a temperature of T, the critical radius r^* is given by the Gibbs–Thomson effect

$$r* = \frac{\gamma}{\rho_s q} \frac{T_m}{T_m - T}, \tag{1}$$

where γ is the solid–liquid interfacial free energy, ρ_s is the solid density, q is the latent heat of melting, and T_m is the bulk melting temperature. With $\gamma = 29 \times 10^{-3}\,\mathrm{J\,m^{-2}}$, $\rho_s = 0.917 \times 10^3\,\mathrm{kg\ m^{-3}}$ and $q = 3.33 \times 10^5\,\mathrm{J\,kg^{-1}}$ [8], we obtain $r^* = 0.026/(T_m - T)$, where r^* is measured in μm. Consequently, the calculated critical diameter at the pores warmer than the growth surface of the warmest ice lens, which had an estimated temperature -0.06°C, is more than 0.87 μm. In addition, ice formation is more difficult in a pore than in bulk water because of surface forces from surrounding

particles [8,12]. The estimated diameter only gives the smallest value and suggests that no ice smaller than about 1 μm exists in pores at positions warmer than the warmest growing ice lens. Therefore, no pore ice exists in any location warmer than the growth surface of the warmest ice lens in the porous medium consisting of glass particles with diameter of 9.7 μm and the ice lens grows without penetrating the warmer pores.

4. Conclusions

Unidirectional freezing experiments were carried out on an unconfined, water saturated, uniform, porous medium consisting of micro glass particles with diameter of 9.7 μm. The formation of ice lenses was observed in the porous medium. The Raman spectrum of water was used to clarify the ice configuration in the vicinity of the growing ice lens. No ice was found in any pore warmer than the warmest ice lens in the porous medium and the ice lens grew without penetrating the warmer pores.

Acknowledgements

The authors wish to thank Dr. Y. Miyata and Mr. Y. Minami for taking the electric micrographs and doing the pore size analysis, Ms. T. Ikeda, Mr. H. Fukazawa and Dr. A. Hori for technical support with the Raman spectroscopy and Dr. M. Fukuda, Dr. T. Hondoh and Dr. T. Ishizaki for advice on our main experiment.

References

[1] J.G. Dash, H.-Y. Fu, J.S. Wettlaufer, Rep. Prog. Phys. 58 (1995) 115.
[2] Y. Muto, K. Watanabe, M. Mizoguchi, T. Ishizaki, Proceedings of the Seventh International Conference on Permafrost, 1998, p. 783.
[3] M. Kumai, CRREL Report, Vol. 79–28, 1979.
[4] S.C. Colbeck, Soil Sci. 139 (1985) 13.
[5] R.D. Miller, Proceedings of the Third International Conference on Permafrost, 1978, p. 377.
[6] R.R. Gilpin, Water Res. Res. 16 (5) (1980) 918.
[7] J.M. Konrad, C. Duguennoi, Water Res. Res. 29 (1993) 3109.
[8] T. Ishizaki, M. Maruyama, Y. Furukawa, J.G. Dash, J. Crystal Growth 163 (1996) 455.
[9] K. Nagashima, Y. Furukawa, J. Crystal Growth 171 (1997) 577.
[10] P.T.T. Wong, E. Whalley, J. Chem. Phys. 62 (1975) 2418.
[11] H. Fukazawa, D. Suzuki, T. Ikeda, S. Mae, T. Hondoh, J. Phys. Chem. B 101 (1997) 6184.
[12] Y.P. Handa, M. Zakrzewski, C. Fairbridge, J. Phys. Chem. 96 (1992) 8594.